Indian Journal of Fundamental and Applied Life Sciences ISSN: 2231– 6345 (Online)
An Open Access, Online International Journal Available at www.cibtech.org/sp.ed/jls/2015/02/jls.htm
2015 Vol. 5 (S2), pp. 1061-1071/Barahmand and Kamali
Research Article

THE NUMERICAL SIMULATION OF TWO-DIMENSIONAL LAMINAR DENSITY CURRENT USING IMMERSED BOUNDARY METHOD NETWORK AND FINITE VOLUME OF POWER LOW SCHEME

***Barahmand N. and Kamali M.**
Department of Civil Engineering, Larestan Branch, Islamic Azad University, Larestan, Iran
**Author for Correspondence*

ABSTRACT
In this study the two-dimensional laminar flow of salt water is coded on an inclined plane as a density current. Accordingly the partial differential equations governing the density current were defragged after being dimensionless using finite volume of power-low scheme. In addition in order to produce the network the immersed boundary method (IBM) was used. Also the solution algorithm of the velocity and pressure fields is the type SIMPLE (*Semi-Implicit Method for Pressure-Linked Equations*) and the equation systems were calculated by SOR (*Successive Over-Relaxation*) iterative technique. For the verification of the written program, the data of Garcia paper was used and the results of simulation in the form of velocity profile were compared with the related laboratory profiles. The results indicate that the calculated values are consistent with the observed results. It was also observed that by reducing the slope of the bed, in any cross section, the maximum velocity of the current is reduced and the maximum current concentration was increased. Finally, it must be noted that hydraulic jump phenomenon was simulated in the bottom of the slopes.

Keywords: *Laminar Density Current, Numerical Modeling, Coding, Immersed Boundary Method*

INTRODUCTION
Density currents are created as a result of the difference between the density of a fluid and another liquid. These currents affect their surrounding environment significantly from the climate change, the formation of clouds and storms to the accumulation of sediments in the reservoir and harm to marine structures. Therefore understanding the density current can help us to understand the consequent events, and provide damage control areas and potential risks. Density currents are the main cause of sediment in reservoirs. However, the process of filling a dam by sediments needs a lot of time but the lack of attention to this phenomenon will reduce the storage capacity of a dam and therefore its useful life and its benefits (Fan and Morris, 1992; Graf, 1984). Research has estimated that each year one percentage of reservoir tank volume is reduced due to the deposition of sediments. These figures alone show the importance of the debates on sedimentation control of the current (Mahmood, 1987).
If we want to consider hydraulic parameters such as velocity and concentration in a density flow, we have three ways: research and field study, the use of physical laboratory models, and finally the use of numerical models. Here the implementation and development of numerical models are less costly than previous methods and their application is not limited to a particular instance. In addition, in numerical models the maneuverability on the geometry of the channel is very high and the channel can be simulated with its original size. Therefore, it is possible to investigate various features simultaneously and without additional costs. Descriptive mathematical models of density currents appeared in late 70s. Theoretical models are widely used for the goals and objectives from the estimation of velocity, current height and sediment particle size distribution to model the structure of turbulence in the density current. Usually these models are created according to the continuity equation of mass and momentum for both fluid and solid phase as well as the diffusion equation (which resents the balance between the rate of changes in suspended materials in controlled volume and the rate of removal of sedimentation in controlled volume). Aram and Firoozabadi (2007)

analyzed permanent salty density currents using laboratory studies. They also simulated the current structure using low-Reynolds numbers turbulence model (Launder and Sharma, 1974). Comparison of the results with experimental data shows the accuracy of turbulence model for three-dimensional density currents (Aram and Firoozabadi, 2007). Kostic and Parker (2006) with the numerical study analyzed the density current characteristics including fine suspended sediments at the reduced slope of the bed (Kostic and Parker, 2006). Also the effects of large-scale roughness (the bed shape) on the properties of turbidity current wan analyzed numerically by Kubo (2004) in the laboratory. It was shown that hydraulic jumps appeared on the density currents on the substrate can increase the settling of suspended sediments in the turbid currents in the downstream area of slope failure (Kubo, 2004). Salaheldin *et al.,* (2004) used the Fluent software for simulating the turbulent flow around a circular vertical base (circular section) in clear water without sediment (Salaheldin *et al.,* 2004). Imran *et al.,* (2004) simulated a three-dimensional density current in a direct channel (using fluent software). It should be noted that the validation of the numerical results was done based on two dimensional experimental data.

They also modeled states that the current is in an enclosed channel (with vertical side walls) and in a non-enclosed channels (with floodplain) (Imran *et al.,* 2004). Lubke *et al.,* (2003) showed that the lateral expansion depends on the degree of nonconformance of turbulent normal stress (Lubke *et al.,* 2003). The one dimensional model of sedimentation in reservoirs was studies in 2003 based on the sedimentation of sand and mud behavior by Toniolo and Parker (2003) and the numerical model was developed (Toniolo and Parker, 2003).

Choi and Garcia (2002) using a modified $K-\varepsilon$ model modeled the buoyancy direction of two-dimensional density currents on an inclined surface (Choi and Garcia, 2002). Firoozabadi *et al.,* (2001) simulated the density currents by a $K-\varepsilon$ turbulence model with low Reynolds number (Launder and Sharma model) (Firoozabadi *et al.,* 2001). Craft and Launder (2001) concluded that the three-dimensional wall jet currents cannot be simulated by $K-\varepsilon$ model (Craft and Launder, 2001). Imran *et al.,* (1998) used an average- deep model to simulate the process of channelization of the alluvial plains below the sea (due to the current density movement). In this model in addition to two-dimensional equations of continuity and fluid momentum the Exert equation of sediment continuity was used (Imran *et al.,* 1998).

Skene *et al.,* (1997) used a model to simulate constant flow and predicted the sediment deposition distribution changes due to topographical obstacles (Skene *et al.,* 1997). Tsihrintzis and Alavian (1996) used a numerical model to simulate the evolution of the density current. It should be noted is that this model was not consistent with experimental data (Tsihrintzis and Alavian, 1996). Farrel and Stefan (1988) created a two-dimensional model for a current density in tanks with simple geometry. They used a $k-\varepsilon$ model to solve the equation (Farrel and Stefan, 1988). It should be noted that similar studies have been conducted by Kupusovic (1989) and Bournet *et al.,* (1999). Parker *et al.,* (1986) created a deep- moderate model in which in addition to usual equations of continuity and fluid momentum the equation of the sediments entering from the bed into the density current was used. In the final equation the deposits entrance term was associated with the amount of turbulence kinetic energy (Parker *et al.,* 1986). Fietz and Wood (1967) conducted experiments on three-dimensional density currents. According to them by getting away from the three-dimensional density current, the stream width increases linearly with distance (Fietz and Wood, 1967).

MATERIALS AND METHODS

Method

In this study the equations of fluid current became dimensionless and then discretize by finite volume of power low scheme. The solution of velocity pressure fields was done using SIMPLE algorithm on a replaced network (Versteeg and Malalasekera, 1995) and in order to solve the equation system the SOR iteration method was used (Richard and Douglas, 1976). For validating the written program the data of Garcia paper was used and the results of simulation in the form of

velocity profile were compared with the related laboratory profiles. The results indicate that the calculated values are consistent with the observed results.

The Equations Governing the Two-dimensional Fluid Current within Cartesian Framework

Continuity Equation

$$\frac{\partial \rho}{\partial t} + \operatorname{div}(\rho \vec{u}) = 0 \tag{1}$$

Since the fluid is incompressible, the term ($\frac{\partial \rho}{\partial t}$) is removed from the equation and the equation is as follows:

$$\frac{\partial u}{\partial x} + \frac{\partial v}{\partial y} = 0 \tag{2}$$

The rate of velocity horizontally:

In general, the equation is as follows:

$$\frac{D(\rho u)}{Dt} = -\frac{\partial p}{\partial x} + \operatorname{div}(\mu \operatorname{grad} u) + S_x \tag{3}$$

The last term in the above equation is the source term. Since there is no force applied on the fluid horizontally, the term is removed. So the two-dimensional equation becomes as follows:

$$\frac{\partial}{\partial t}(\rho u) + \frac{\partial}{\partial x}(\rho u u) + \frac{\partial}{\partial y}(\rho v u) = -\frac{\partial p}{\partial x} + \frac{\partial}{\partial x}\left[\mu \frac{\partial u}{\partial x}\right] + \frac{\partial}{\partial y}\left[\mu \frac{\partial u}{\partial y}\right] \tag{4}$$

The rate of vertical velocity:

$$\frac{D(\rho v)}{Dt} = -\frac{\partial p}{\partial y} + \operatorname{div}(\mu \operatorname{grad} v) - g(\rho - \rho_0) + S_y \tag{5}$$

By expanding the terms the equation is as follows:

$$\frac{\partial}{\partial t}(\rho v) + \frac{\partial}{\partial x}(\rho u v) + \frac{\partial}{\partial y}(\rho v v) = -\frac{\partial p}{\partial y} + \frac{\partial}{\partial x}\left[\mu \frac{\partial v}{\partial x}\right] + \frac{\partial}{\partial y}\left[\mu \frac{\partial v}{\partial y}\right] - g(\rho - \rho_0) + S_y \tag{6}$$

In the above equation $-g(\rho - \rho_0)$ is the buoyant term. In this equation ρ_0 is the reference density.

The relationship between density changes and concentration about buoyancy term is calculated from the following relationship:

$$\rho = \rho_0 + \left(\frac{\partial \rho}{\partial C}\right)_P (C - C_0) \tag{7}$$

By replacing the above equation and assuming that the fluid is incompressible, equation (6) is written as follows:

$$\frac{\partial v}{\partial t} + \frac{\partial uv}{\partial x} + \frac{\partial vv}{\partial y} = -\frac{1}{\rho}\frac{\partial p}{\partial y} + \frac{\partial}{\rho \partial x}\left[\mu \frac{\partial v}{\partial x}\right] + \tag{8}$$

$$\frac{\partial}{\rho \partial y}\left[\mu \frac{\partial v}{\partial y}\right] + g\left[-\frac{1}{\rho}\left(\frac{\partial \rho}{\partial C}\right)_P (C - C_0)\right] + S_y$$

Volume- mass expansion coefficients are defined as follows:

$$\beta_m = -\frac{1}{\rho}\left(\frac{\partial \rho}{\partial C}\right)_P \tag{9}$$

By replacing these two definitions in equation (8) this equation is changed into the following equation:

$$\frac{\partial v}{\partial t}+\frac{\partial uv}{\partial x}+\frac{\partial vv}{\partial y}=-\frac{1}{\rho}\frac{\partial p}{\partial y}+\frac{\partial}{\rho\partial x}\left[\mu\frac{\partial v}{\partial x}\right]+\frac{\partial}{\rho\partial y}\left[\mu\frac{\partial v}{\partial y}\right]+g\left[\beta_m\left(C-C_0\right)\right] \quad (10)$$

By increasing the concentration of salt the fluid density increases. Thus, according to the relationship (9) the value of β_m must be negative. Usually the negative sign of β_m is entered into equation (10) and consider the amount of volume-mass expansion coefficient positive. The value of (C_0) is considered equal to zero which means that it is considered in the top layer. Therefore the final equation of motion in the vertical direction is as follows:

$$\frac{\partial v}{\partial t}+\frac{\partial uv}{\partial x}+\frac{\partial vv}{\partial y}=-\frac{1}{\rho}\frac{\partial p}{\partial y}+\frac{\partial}{\rho\partial x}\left[\mu\frac{\partial v}{\partial x}\right]+\frac{\partial}{\rho\partial y}\left[\mu\frac{\partial v}{\partial y}\right]+g\left[-\beta_m C\right] \quad (11)$$

Mass Transfer Equation

In order to model the process of salt distribution Fick's law is devised. The two-dimensional mass transfer equation is as follows:

$$\frac{\partial C}{\partial t}+\frac{\partial uC}{\partial x}+\frac{\partial vC}{\partial y}=D\left[\frac{\partial^2 C}{\partial x^2}+\frac{\partial^2 C}{\partial y^2}\right]+S_c \quad (12)$$

Where D is diffusion coefficient and S_c is the source term.

Providing Network by Immersed Boundary Method

Immersed boundary methods were initially used by Peskin (1972) to simulate blood flow in the heart. Peskin used this method to model heart's elastic valve. The main feature of this method is current analysis in Cartesian network which is inconsistent with the geometry of the object. In other words, regardless of the geometry of the body, the governing equations are discretized and solved on arbitrary networks (often Cartesian). In order to better describe the method Figure 1 is considered. The traditional method of solving the current on this object is to use a network in accordance with the geometry of the object (Figure 2). The creation of this network (structured or unstructured) consists of two stages. In the first stage a surface network that covers Γ_b is produced. Then in the next step this surface network is used as the boundary condition to produce network in the whole field.

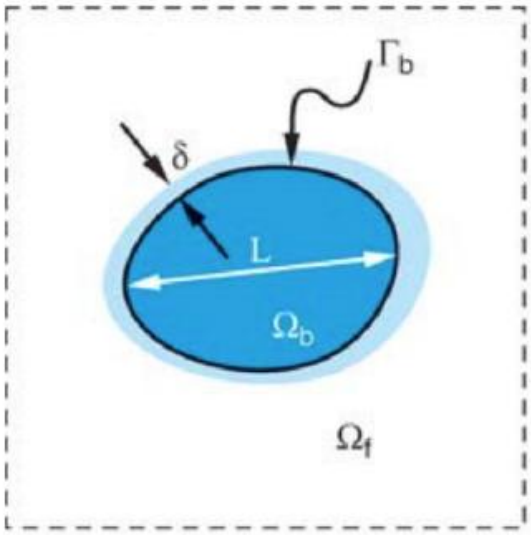

Figure 1: The schematic of the problem

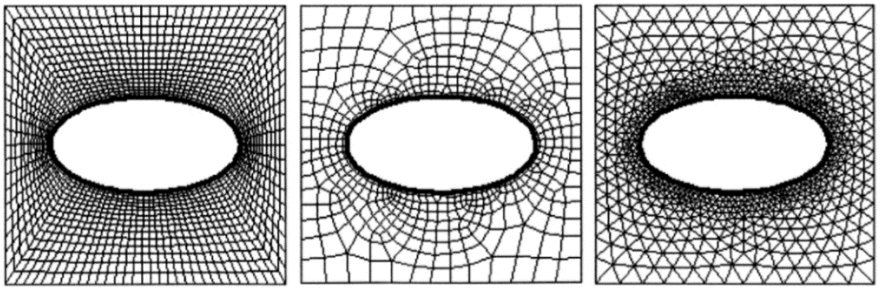

Figure 2: Networks matching the figure's core

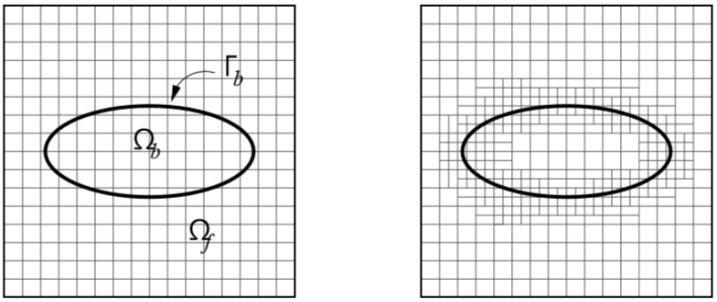

Figure 3: Network created by the immersed boundary

Figure 3 presents the reaction of the immersed boundary to this problem. As it is clear in the figure a network inconsistent with the object geometry is formed on the object to analyze the current on the object. Obviously the lack of compliance of the object's boundary with the network nodes cancels the possibility of application of the boundary conditions on nodes. Therefore, measures must be taken to apply the boundary conditions on the network inconsistent with the geometry of the object. Adding a source term to the momentum equation, Peskin provided this condition. The method of calculating the source term or the boundary conditions in immersed boundary method has led to the appearance of a variety of methods.

To learn about immersed boundary methods, the incompressible current around is considered around the object 3. The equations of such a process are:

$$\frac{\partial \vec{u}}{\partial t} + \vec{u}.\vec{\nabla u} + \frac{1}{\rho}\nabla p - \frac{\mu}{\rho}\nabla^2 \vec{u} = 0 \quad (13)$$

$$\vec{\nabla}.\vec{u} = 0 \qquad \text{in} \qquad \Omega_f \quad (14)$$

$$\vec{u} = \vec{u}_\Gamma \qquad \text{in} \qquad \Gamma_b \quad (15)$$

Where, $\vec{u}$ is the fluid velocity, p Fluid pressure, ρ Fluid density, μ fluid viscosity. The solid object has occupied Ω_b area and its boundary is determined by Γ_b. Ω_f represents the flow field around the body. In order to facilitate the conceptual description of the methods, the above equation can be rewritten as a system of equations:

$$L(\underline{U}) = 0 \qquad \text{in} \qquad \Omega_f \quad (16)$$

$$\underline{U} = U_\Gamma \qquad \text{in} \qquad \Gamma_b \quad (17)$$

Where $\underline{U} = (\vec{u}, p)$ and L is the operator that represents Navier-Stokes equations.

In the immersed boundary method, equation (13) is discretized on a Cartesian network inconsistent with the geometry of the object and the boundary conditions are applied indirectly by modifying the

equation (16). Generally these modifications are added to the main equation as a source term. There are two general methods to implement this source term. In the first method the source term which is presented by $\underline{f}_b$ is added to the equations. Therefore equation (16) becomes as follows:

$$L(\underline{U}) = f_b \tag{18}$$

Then equation (24) is applied to the whole solution field. Then this equation is discretized on Cartesian network. In the second method, the equations on Cartesian network are discretized and then around the immersed boundary these equations are modified. The first methods in which the source term is added to the equation and then the equations are discretized on the whole field are called Continuous forcing approaches. The second methods in which the equations are discretized on the whole field and then modified around the immersed boundary by adding the source term are called Discrete forcing approach (ReinoutvanderMeˆulen, 2006; Rajat and GianlucaIaccarino, 2005).

Velocity Boundary Conditions

In general, the walls of the current are fixed walls and the condition of lack of slip is true about them. These walls are impermeable and there is no surface perpendicular to them. About the computational cells of the horizontal speed adjacent to eastern and western boundaries they are not disconnected from the boundary. Similarly the vertical speed computational cells in northern and southern boundaries are not disconnected from the boundary. So it is possible to use the discrete equations of velocity in horizontal and vertical directions for these boundaries. The northern boundary of the surface which is the water surface is considered regardless of the air borders without shear stress. This boundary is assumed to be impermeable as well. According to the above velocity boundary conditions are as follows:

$$U = 0 \qquad at \qquad Y = 0$$

$$\frac{\partial U}{\partial Y} = 0 \, at \qquad Y = L$$

$$V = 0 \qquad at \qquad X = 0 \;\; and \;\; X = W$$

The effect of these boundary conditions on the first computational cell adjacent to the boundary in question is involved and they are entered into the equation as the source term. The adjacent cells to different boundaries are presented in Figure 4 and 5.

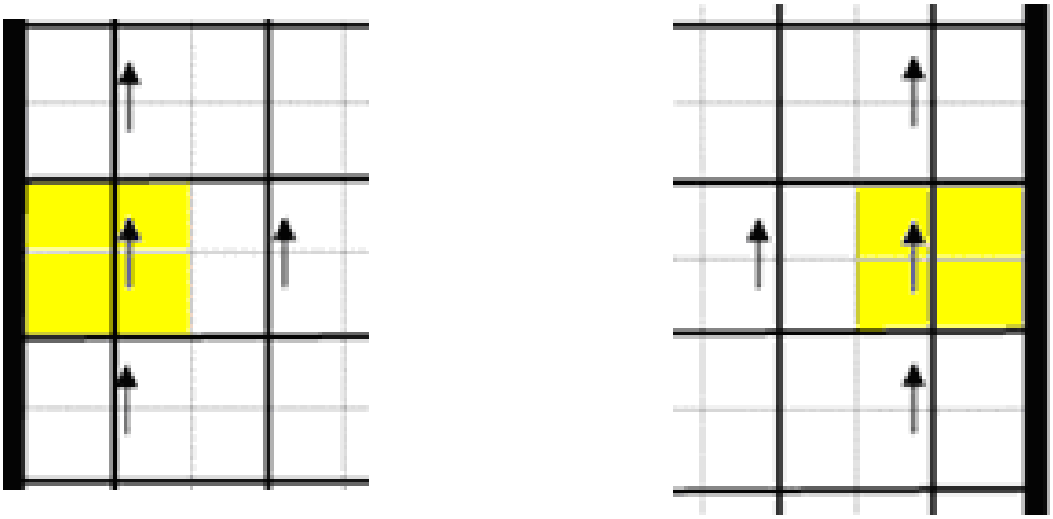

A **B**

Figure 4: Vertical velocity cells adjacent to eastern boundary (Figure A) and western boundary (Figure B) or the calculation area

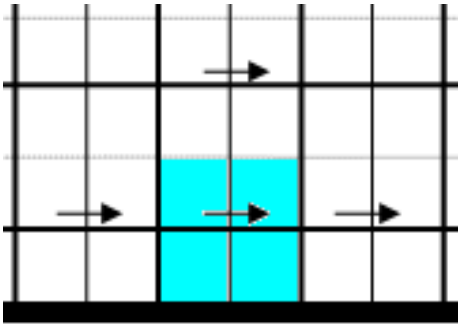

Figure 5: The horizontal velocity calculation cell adjacent to southern boundary, current bed

Concentration Boundary Conditions

In this study it is assumed that the reservoir is filled with fresh water. Concentration in this sense means a constant concentration equal to zero. In terms of the correctness of this condition it should be noted that due to the greatness of Schmidt number (Sc) in case of salt water, some sources do not consider any compensation boundary of concentration reduction in the lower level and a boundary with constant zero concentration in the top transfer layer for the numerical problem and it has been shown that the distribution process is so slow that has no effect on the solution of the problem for the velocity variables. The walls are also assumed impermeable to salt which is fully consistent with reality.

The concentration (C) has the maximum amount in the input valve. The boundary conditions of the concentration equation are as follows:

$$\frac{\partial C}{\partial X}=0 \qquad at \qquad X=0 \ and \qquad X=W$$

$$C=1 \qquad at \qquad Y=0$$

$$C=0 \qquad at \qquad Y=L$$

Boundary conditions affect the discrete concentration equation of the first adjacent cell and enter into it as the source term.

RESULTS AND DISCUSSION

After coding with changing each one of the primary parameters of slope, velocity and concentration, their effect of flow behavior has been investigated. The conditions of the base optional current are presented in Figure 6 and Table 1.

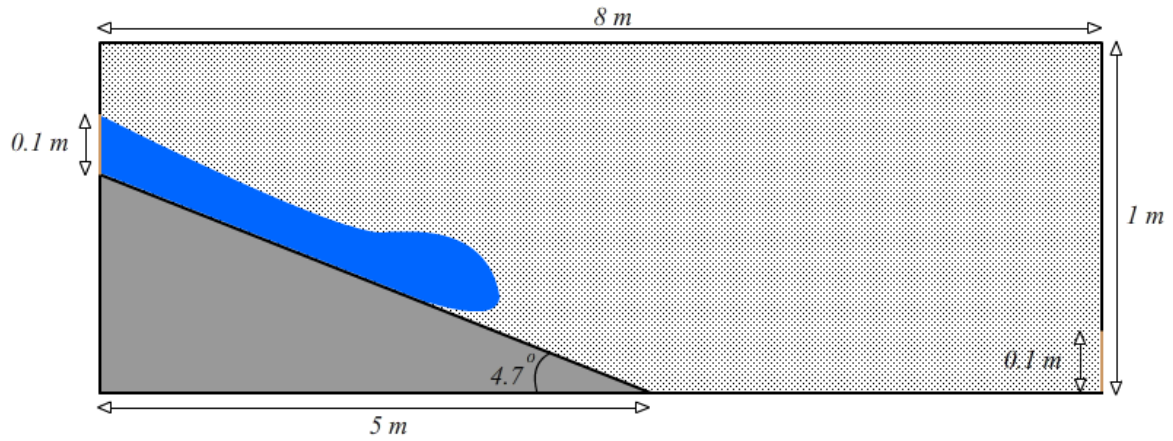

Figure 6: Schematic of density current

Table 1: Characteristics of the base flow

Height (m)	Length (m)	Inlet Height (m)	Outlet Height (m)	Slip Length (m)	Slip Angle (θ°)	U (m/s)	C	Re	Sc
1	8	0.1	0.1	5	4.7	0.11	1	1000	1

The Impact of Changes in the Slope on Velocity and Concentration Profiles

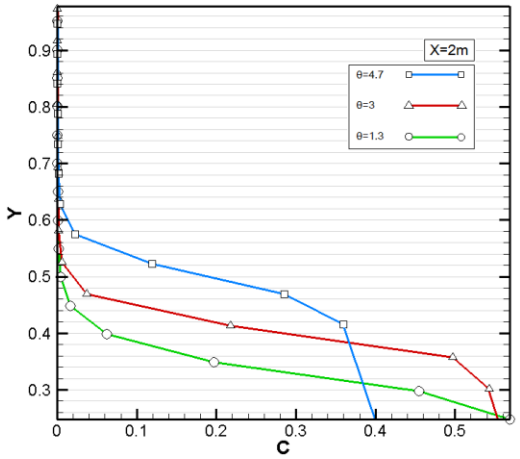

Figure 7: Concentration profile in different slopes

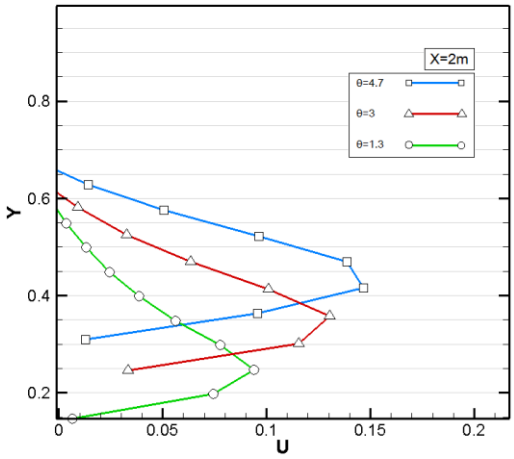

Figure 8: Velocity profile in different slopes

Table 2: The impact of the change in angle on maximum concentration and velocity of the current

Bed Angle	θ = 4.7 °	θ = 3 °	θ = 1.3 °
Maximum speed	0.147	0.129	0.094
Percent change	-----	-12.24	-36.05
Maximum concentration	0.4	0.55	0.57
Percent change	-----	37.5	42.5

The results of Figure 7, 8 and Table 2 show that with Reducing the slope of the bed the maximum velocity reduced and the maximum concentrations are increased.

The Impact of Changes in the Input Concentration on Velocity and Concentration Profiles

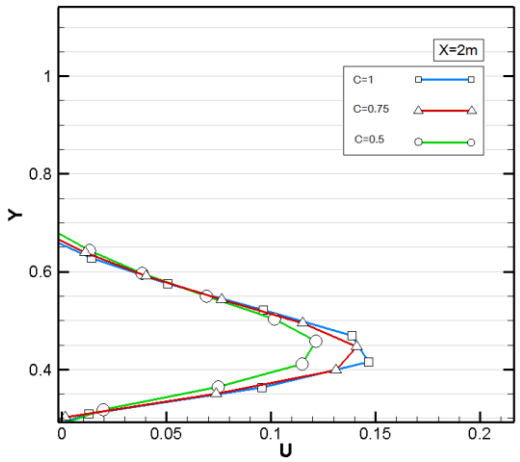

Figure 9: Velocity profile in different input concentrations

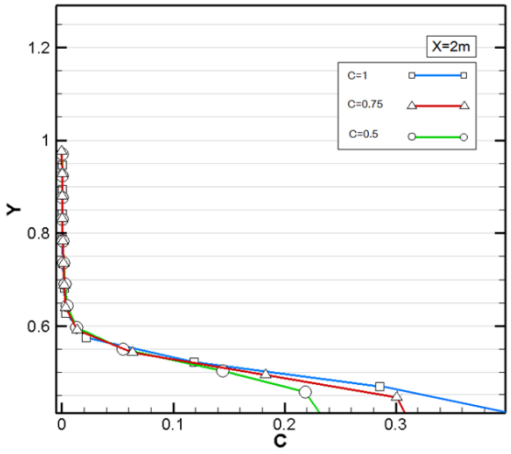

Figure 10: Concentration profile in different input concentrations

Table 3: The impact of the change in concentration on maximum concentration and velocity of the current

Input concentration	C = 1	C = 0.75	C = 0.5
Maximum speed	0.147	0.14	0.12
Percent change	-----	-4.76	-18.36
Maximum concentration	0.4	0.31	0.23
Percent change	-----	-22.5	-42.5

The results of Figure 9, 10 and Table 3 show that with reducing input concentration the maximum concentrations and velocity are reduced.

The Impact of Changes in the Input Velocity on Velocity and Concentration Profiles

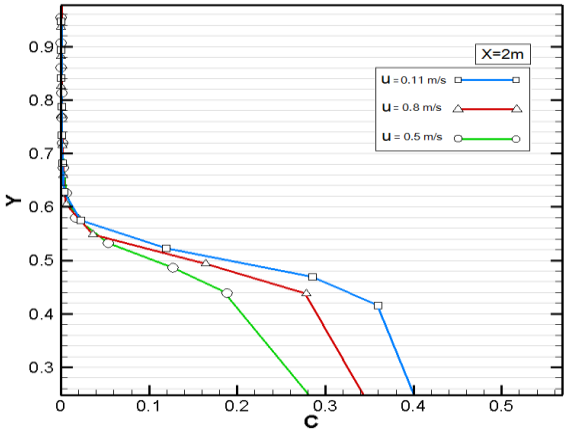

Figure 11: Concentration profile in different input velocity

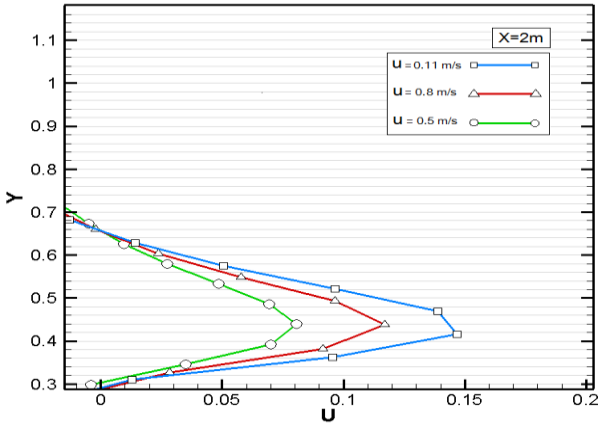

Figure 12: Velocity profile in different input velocity

Table 4: The impact of the change in input velocity on maximum concentration and velocity of the current

Input velocity	U = 0.11	U = 0.8	U = 0.5
Maximum speed	0.147	0.116	0.08
Percent change	-----	-21.08	-45.57
Maximum concentration	0.4	0.34	0.28
Percent change	-----	-20	-30

The results of Figure 11, 12 and Table 4 show that with reducing input velocity the maximum concentrations and velocity are reduced.

Velocity and Altitude Changes versus the Distance from the Current Input

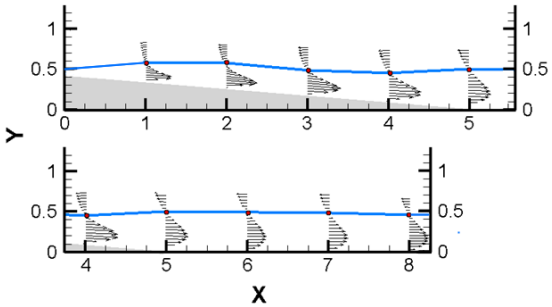

Figure 13: The diagram of current height and velocity vectors at different sections of the reservoir

According to the current height diagram in Figure 13 it can be observed that the current velocity becomes maximum before reaching the end of the inclined plane.

Conclusion

By changing the input parameters of the current such as slope, concentration and velocity and analyzing their effects in different stated the following results were obtained:

- Reducing the slope of the bed reduces the maximum current velocity. So that by changing the bed angle from 4.7 degrees to 1.3 degrees the maximum velocity is reduced by 36% (Table 2)
- Reducing the slope of the bed increases the maximum concentration. According to Table 2 by changing the angle from 4.7 degrees to 1.3 degrees the maximum concentration is increased by 57%.
- Reducing the input concentration reduces the maximum current velocity. So that by changing the input concentration from 1 to 0.5 the maximum velocity is reduced by 18% (Table 3).
- Reducing the input concentration reduces the maximum concentration. According to Table 3 by changing the input concentration from 1 to 0.5 the maximum concentration is reduced by 42%.
- Reducing the input velocity reduces the maximum current velocity. So that by changing the input velocity from 0.11 to 0.5 m/s the maximum velocity is reduced by 46% (Table 4).
- Reducing the input velocity reduces the maximum concentration. According to Table 4 by changing the input velocity from 0.11 to 0.5 m/s the maximum concentration is reduced by 30%.
- A small negative current is formed above the level of density current (Figure 13)
- The current velocity becomes maximum before reaching the end of the inclined plane. But at the end of the inclined plane the current velocity is reduced and the current height increases and hydraulic jump occurs (Figure 13).

REFERENCES

Fan J and Morris GL (1992). Reservoir sedimentation. I: Delta and density current deposits. J. Hydraul. Eng., **118**(3) 354–369.

Graf WH (1984). Storage losses in reservoirs. Int. Water Power and Dam Constr., **36**(4).

Mahmood K (1987). Reservoir sedimentation: Impact, extent and mitigation. Technical paper No.71, The World Bank, Washington D.C.

Aram E and Firoozabadi B (2007). Numerical Simulation and Experimental Investigation of 3-Dimensional Confined Density Currents. *International Journal of Dynamics of Fluids* **3**(1) 45-62.

Kostic S and Parker G (2006). The response of turbidity currents to a canyon-fan transition: internal hydraulic jumps and depositional signatures. J. Hydraul. Res., **44**(5) 631-653.

Kubo Y (2004). Experimental and numerical study of topographic effects on deposition from two-dimensional, particle-driven density currents. *Sedimentary Geology* **164** 311-326.

Salaheldin TM, Imran J and Chaudhry H (2004). Numerical Modeling of Three-Dimensional Flow Field around Circular Piers. *Journal of Hydraulic Engineering* **130**(2) 91-100.

Imran J, Kassem A and Khan SM (2004). Three-dimensional modeling of density current. I. Flow in straight confined and unconfined channels. J. Hydraul. Res., **42**(6) 578–590.

Lubke HM, Rung Th and Thiele F (2003). Prediction of the Spreading Mechanism of 3D Turbulent Wall Jets with Explicit Reynolds-Stress Closure. Int. J. Heat and Fluid Flow., **24** 434–443.

Toniolo H and Parker G (2003). 1D numerical modeling of reservoir sedimentation. *Proceedings of IAHR Symposium on River, Coastal and Estuarine Morphodynamics, Barcelona, Spain* 457-468.

Choi SU and Garcia MH (2002). $k-\varepsilon$ turbulence modeling of density currents developing two dimensionally on a slope. J. Hydraul. Eng., **128**(1) 55-63.

Firoozabadi B, Farhanieh B and Rad M (2001). The Propagation of Turbulent Density Currents on Sloping Bed. J. Scientia of Iranica., **8**(2) 223–235.

Craft TJ and Launder BE (2001). On the Spreading Mechanism of the Three- Dimensional Turbulent Wall Jet. J. Fluid Mechanics., **435** 305– 326.

Imran J, Parker G and Katopodes N (1998). A numerical model of channel inception on submarine fans. J. Geophys. Res., **103**(c1) 1219–1238.

Skene KI, Mulder T and Syvitski JPM (1997). INFLO1: a model predicting the behavior of turbidity currents generated at river mouths. Comput. Geosci., **23** 975– 991.
Tsihrintzis VA and Alavian V (1996). Spreading of Three- Dimensional Inclined Gravity Plumes. *Journal of Hydraulic Research* **34**(5) 695–711.
Farrel GJ and Stefan H (1988). Mathematical modeling of plunging reservoir flows. *Journal of Hydraulic Research* **26**(5) 525–537.
Kupusovic T (1989). A Two Dimensional Model of Turbulent Flow Applied to Density Currents, *Proceedings of Computational Modeling and Experimental Methods in Hydraulics (HYDROCOMP'89)* (Elsevier Applied Science) England.
Bournet P, Dartus D, Tassin B and Vincon-Leite B (1999). Numerical investigation of plunging density current. J. Hydraul. Eng., **125**(6) 584–594.
Parker G, Fukushima Y and Pantin HM (1986). Self-accelerating turbidity currents. J. Fluid Mech., **171** 145-181.
Fietz TR and Wood IR (1967). Three-dimensional density current. *ASCE Journal of Hydraulics Division* **93**(HY6) 1–23.
Versteeg HK and Malalasekera W (1995). An introduction to computational fluid dynamics. *The Finite Volume Method* 85-154.
Richard L Burden and Douglas Faires J (1976). *Numerical Analysis,* ninth edition 462-469.
Marcelo H Garcia (1992). Hydraulic Jumps in Sediment-Driven Bottom Currents. *Journal of Hydraulic Engineering* **119**(10) 1094-1117**.**
ReinoutvanderMeˆulen (2006). *The Immersed Boundary Method for the (2D) Incompressible Navier-Stokes Equations* 7-19.
Rajat Mittal and GianlucaIaccarino (2005). Immersed boundary methods. Annu. Rev. Fluid Mech. **37** 239-261.